Emission spectra from single rovibronic quantum states in S_1 benzene after Doppler-free two-photon excitation

U. Schubert, E. Riedle, and H. J. Neusser
Institut für Physikalische und Theoretische Chemie, Technische Universität München, Lichtenbergstr. 4, D-8046 Garching, West Germany

(Received 3 November 1988; accepted 25 January 1989)

Dispersed emission from single rovibronic quantum states in S_1 benzene is measured after Doppler-free two-photon excitation under low pressure conditions (0.3 Torr). This was made possible by a long-term stabilization of the single-mode dye laser yielding a stability of better than 1 MHz/h. The emission spectra of unperturbed rotational levels in the 14^1 and the $14^1 1^1$ vibronic states reveal a great number of detailed results on Duschinsky rotation and long-range Fermi resonances in the electronic ground state. By contrast, it is seen that the emission spectra from perturbed rovibronic states are contaminated by additional bands. The analysis of these bands leads in most cases to an identification of the coupled dark background state and the responsible rotation–vibration coupling process (H_{42} resonances). The emission spectra clearly demonstrate that even for a density of states of 60 $1/cm^{-1}$, coupling in S_1 benzene is still selective and far from the statistical limit. It is further demonstrated that the dark and the light states are more efficiently mixed by short-range couplings with coupling matrix elements of some GHz than by long-range Fermi resonances.

I. INTRODUCTION

One of the first indications of an intramolecular vibrational redistribution process (IVR) in large polyatomic molecules emerged from the observation of emission spectra under collision-free conditions. Experiments were performed on benzene,[1,2] para-difluorobenzene,[3] and naphthalene.[4] Dispersed emission spectra were measured after excitation of vibrational quantum states at different excess energies in the S_1 electronic state. While the emission spectra from low energy vibrational states reflected the identity of the excited state as expected, a striking result was found for vibrational states at high excess energy. A broad background (grass) appeared in the spectra. This was attributed to an energy redistribution process onto the numerous vibronic modes of the molecule which takes place after the initial excitation of the vibrational state. Since the resolution of excitation was limited to several 10 cm^{-1} (Ref. 1) in the early experiments it was not clear whether a pure vibrational state was prepared and to what degree hot band excitation contributed to the background.[4] Later on it has been shown by the application of cooled supersonic jet techniques that hot band excitation alone could not account for the observed background.[5,6] Despite the inherent problem of rather limited resolution emission spectra still present a very direct and visual picture of the coupling processes leading to IVR in large molecules.[7,8]

From the emission spectra the *existence* of energy redistribution processes in large systems could be concluded. However, to learn about the *mechanisms* responsible for IVR, experiments were desirable which provided a higher precision in the selection of the initial state. In recent work we have shown that Doppler-free two-photon excitation with a resolution of 100 MHz or better enables one to selectively excite single quantum states even in large molecules the size of benzene.[9] Homogeneous linewidths[10] and decay times of single defined rovibrational quantum states[11] have been measured for the first time with this technique. Furthermore, the selective coupling of the excited light zero-order state to a dark zero-order background state in S_1 was observed and the resulting quasieigenstates, split by several 100 MHz, were resolved in the high-resolution spectra.[12] All experimental results revealed a distinct J,K dependence of the linewidths, lifetimes, and splittings and indicated that vibration–rotation coupling plays a dominant role in the process leading to IVR in benzene. The precision and selectivity of the Doppler-free high resolution excitation on the one hand and the perspicuity of dispersed emission spectroscopy on the other hand suggest to combine both techniques. In this work we will show that indeed this combination is possible. We will present the first example of dispersed emission spectra originating from single rovibronic quantum states in a large polyatomic system.

It will be shown that the nature of the coupled dark background states can be directly elucidated by these experiments. More important, it is seen, that within one vibronic state of low excess energy, different rotational states are coupled to different background states. As a consequence, the character of the emission spectrum can change drastically when the excitation energy is changed by only 0.01 cm^{-1} within the rotational contour of a vibronic band. These short-range couplings giving rise to local perturbations within the vibronic band are thought to be responsible for dynamic IVR at higher excess energies. Experimental results are reported for various rotational states in the 14^1 and $14^1 1^1$ vibronic states of benzene, C_6H_6 and C_6D_6.

II. EXPERIMENTAL

The scheme of the experimental setup is shown in Fig. 1. It consists of a tunable cw ring dye laser (Coherent CR 699)

 0021-9606/89/115994-14$02.10

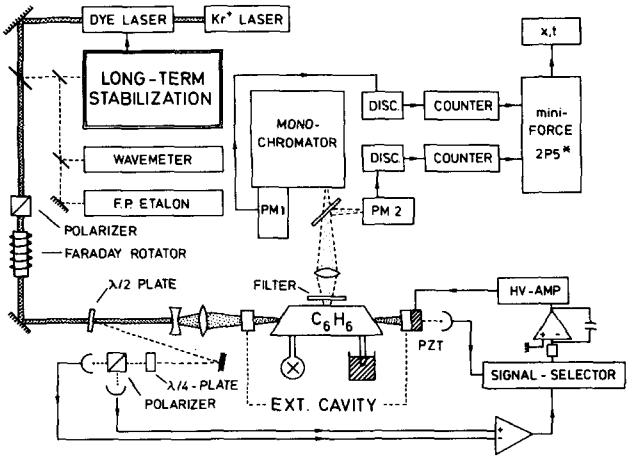

FIG. 1. Experimental setup for the measurement of the dispersed fluorescence from individual rotational levels in the 14^1 and $14^1 1^1$ vibronic levels of benzene. The frequency resolved one-photon emission is observed after Doppler-free two-photon excitation of C_6H_6 (C_6D_6) in an external cavity. The long-term laser stabilization guarantees a stability of the excitation frequency within $\pm$ 1 MHz during the monochromator scan.

pumped by a Kr^+ laser. The frequency width is 1 MHz and the light power around 5000 Å is about 350 mW. The laser light is fed into an external cavity which leads to a 30-fold increase of the intensity of the standing wave light field needed for Doppler-free two-photon excitation.[10] The cell containing benzene vapor under a pressure of typically 300 mTorr is placed within the external cavity. Elimination of the Doppler broadening is achieved by the absorption of two photons propagating in opposite direction in the standing wave field of the external resonator. The external cavity is locked to the laser frequency by a Hänsch–Coulliaud method[13] as shown schematically in Fig. 1. The UV fluorescence originating from the excited single rovibrational two-photon state of benzene is collimated onto the entrance slit of a 1.25 m Czerney–Turner spectrometer (Spex Model No. 1269) and a photomultiplier at the exit slit detects the dispersed emission. The spectrometer is used in the second order of the grating. This means that any visible stray light (reflected in the first order) is seen at half the wavelength in the emission spectrum. Typically, a frequency scan of 5000 cm^{-1} takes about 30 min due to the low intensity of the emitted light. During that time the laser frequency has to be stable within $\pm$ 1 MHz in order to stand just on the top of the selected sharp two-photon line [$\approx$7 MHz full width at half maximum (FWHM)] and to guarantee constant excitation conditions for different parts of the emission spectrum. A long-term stabilization was developed to meet these experimental demands. Its details are described elsewhere.[14] Briefly, it consists of a home-built, highly stable, evacuated, and temperature-controlled Zerodure interferometer which provides frequency standards at every 150 MHz. The laser frequency is locked to one of these standards, but in addition, it can be tuned over a range of about 200 MHz with an acousto-optic modulator. In this way the laser frequency can be tuned to any selected two-photon line and be kept there with a stability of <1 MHz/h. The photons monitored by the photomultiplier are counted and the signal is transferred to a minicomputer (Force 2P5). Part of the undispersed total UV emission is monitored with a second photomultiplier. In this way long-term changes in the laser power and/or laser frequency can be detected.

III. RESULTS AND DISCUSSION

A. Doppler-free two-photon spectrum of the 14_0^1 band

Recently the rotational lines of the 14_0^1 two-photon band in benzene, C_6H_6, have been completely resolved. More than 3000 individual lines have been assigned and the rotational and quartic centrifugal distortion constants of the band were determined with high accuracy.[15,16] Several localized perturbations were analyzed in the rotational contour[16] and it was found that the decay time of the perturbed states is considerably shorter than the decay time of the unperturbed states.[11] A similar analysis has been performed for perdeuterated benzene, C_6D_6.

In Fig. 2 part of the Q branch of the 14_0^1 band in C_6H_6 is shown. Several of the rotational lines are marked by an arrow and the final state assignment of the corresponding transition is given. For these states, emission spectra have been measured. Final states indicated by a and b are the quasieigenstates resulting from a coupling process of the light zero-order state to a dark background state. Their positions were found to be shifted from the calculated position of the corresponding zero-order state. The analysis of the residuals yields the avoided crossings curves shown in Fig. 3. The high resolution of Doppler-free two-photon excitation and the good signal-to-noise ratio makes possible the identification of very low intensity perturbed lines. As a result, the observation of both quasieigenstates resulting from the mixing of the zero-order states is possible for a wide range of J values around the crossing point (see Fig. 3). From the exact position of the eigenstates the coupling matrix element of each pair can be determined as a function of J and constant K quantum numbers.

The information on the coupling process between light and dark zero-order states discussed so far has been found from an analysis of line positions in the two-photon excitation spectrum. The unperturbed and perturbed character and the identity of the coupled background states will now be investigated from the dispersed emission of selected states.

B. Emission spectra from single rotational states in the 14^1 state

1. Unperturbed states

Emission spectra were first measured for unperturbed rotational states in the 14^1 vibronic state of C_6H_6 and C_6D_6 at a vibrational excess energy of 1571 and 1567 cm^{-1}, respectively. The laser frequency was scanned to the maximum of the selected individual two-photon line and locked to this frequency by the technique described in Sec. II. Then the emission spectrum was measured.

a. 9_9 state in C_6H_6. In Fig. 4 the UV emission spectrum resulting from the $14^1, J'_{K'} = 9_9$ state of C_6H_6 at a resolution of 20 cm^{-1} is shown. The strong peak on the right-hand side

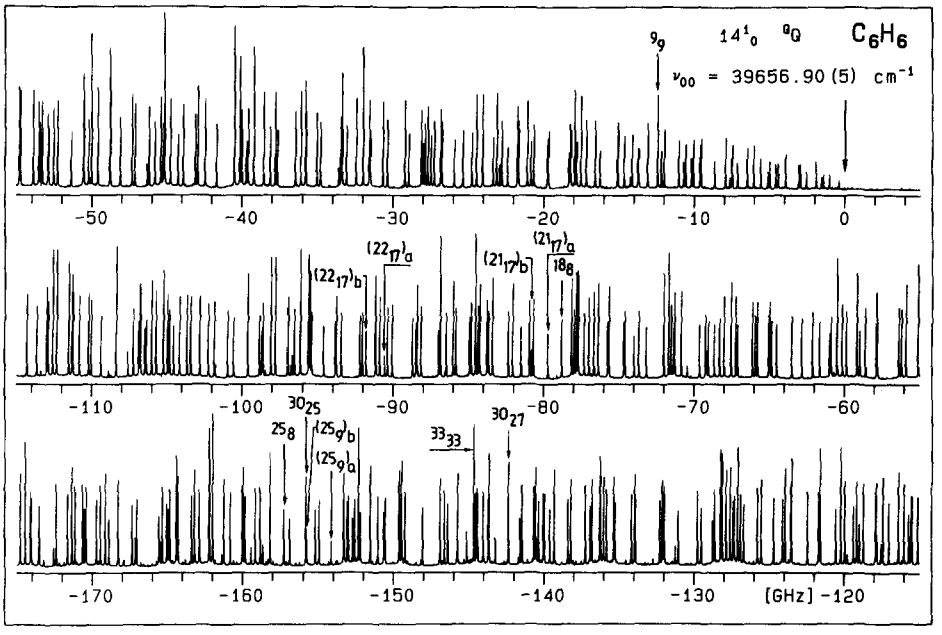

FIG. 2. Blue part of the Q branch of the 14^1_0 two-photon excitation spectrum of C_6H_6. Transitions which have been selected for measurement of dispersed fluorescence are indicated.

of the spectrum marked by an asterisk results from stray light of the exciting visible light (19 828 cm^{-1}) which gives rise to a peak at the apparent frequency of 39 652 cm^{-1}. This is due to the fact that the visible light is observed in the first order of the grating, while the UV emission is seen in the second order. The peak serves for absolute calibration of the frequency scale to a precision of better than 10 cm^{-1}. The emission spectrum consists of three strong peaks and several additional small features. It is well separated from the stray light peak since the absorption mechanism (two-photon) is different from the emission process (one-photon) and the inducing modes ν_{14} of the two-photon-absorption and ν_6 of the one-photon-emission differ strongly in frequency.

(i) The dominant features are readily assigned as the expected $14^1_i 6^0_1 1^0_n$ progression bands.[17] The appearance of one quantum of ν_6 in the final state is necessary to induce the one-photon emission from the S_1, 14^1 vibronic state. The intensity ratio of the four ν_1 progressions observed is close to that found for emission spectra from the 0^0 state.[18]

(ii) Most of the small peaks in the spectrum are due to other inducing vibrations for the one-photon emission. This is analogous to the additional bands in the emission spectrum from the 0^0 level observed by Parmenter and coworkers.[1,19] Both the 0^0 level as well as the 14^1 level do not contain a one-photon inducing mode and thus the one-photon emission has to be induced by suitable vibrations. The resulting transitions which are observed in the spectrum of Fig. 4 are $14^1_i 16^0_2$, $14^1_i 10^0_2 6^0_1$, $14^1_i 11^0_1 16^0_1$, $14^1_i 9^0_1$, $14^1_i 10^0_2$, $14^1_i 17^0_2$, $14^1_i 7^0_1$. The vertical lines at the bottom of the spec-

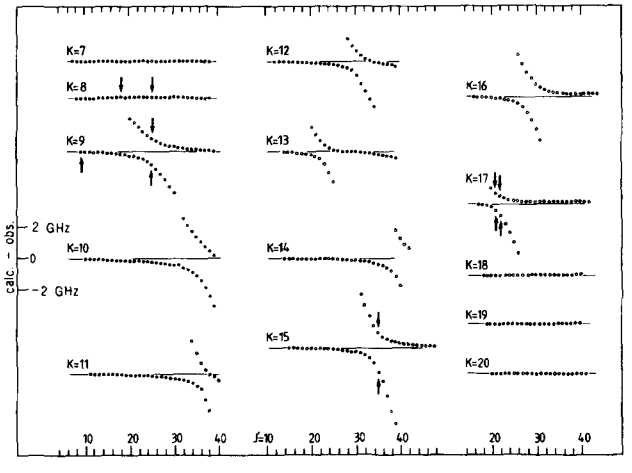

FIG. 3. Residuals found from the analysis of line positions in the 14^1_0 band of C_6H_6 (taken from Ref. 16). The arrows indicate the states whose emission spectra were measured.

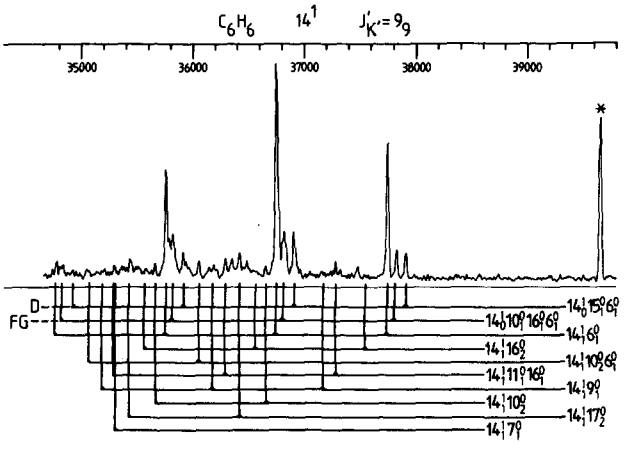

FIG. 4. Single rovibronic level emission spectrum of the rotational state $J'_{K'} = 9_9$ in the vibronic level 14^1 of C_6H_6. The peak produced by laser stray light in the first order of the grating is marked by an asterisk. It represents the two-photon excitation energy. The vertical markers indicate the calculated transition frequencies of the assigned transitions. Transitions denoted by D are due to Duschinsky rotation of the ν_{14} and ν_{15} normal coordinates in the excited (S_1) state vs the ground (S_0) state. FG indicates long-range Fermi resonances in the S_0 state. 1^0_n has to be added to every assignment and indicates the observed progression members due to the ν_1 (a_{1g}) vibration.

trum mark the expected transition frequencies of these bands when calculated from the harmonic vibrational frequencies.[20] It is seen that they agree well with the experimentally observed peak positions and it is further seen that nearly all peaks, even in the somewhat congested range of the spectrum below 37 000 cm^{-1}, can be assigned.

(iii) The two distinct peaks to the blue of the dominant $14_1^1 6_1^0$ band need a more detailed discussion. They are not present in the emission spectrum from the 0^0 level in Refs. 1 and 19. Obviously, they are typical for the additional ν_{14} vibration in both the excited and the ground state of the one-photon emission band. The peak 74 cm^{-1} to the blue of the $14_1^1 6_1^0$ band can be assigned on the basis of our previous hot band two-photon spectra.[21] In these spectra a surprisingly strong $16^0_1 10^0_1$ band was observed. We concluded that it gains its intensity from long-range anharmonic coupling of the $10_1 16_1$ state (1245 cm^{-1}) to the 14_1 state (1309 cm^{-1}) (FG) rather than by second-order Herzberg–Teller coupling of the two-photon transition. This previous conclusion is confirmed by the appearance of the $14_0^1 10_1^0 16_1^0 6_1^0$ emission band in Fig. 4. From the two-photon hot band spectrum it is known that there is a frequency shift of 18 cm^{-1} of the $10_1 16_1 6_1$ state which was supposed to be due to the Fermi resonance. In Fig. 4 the transition frequency to an unperturbed $16_1 10_1$ state is marked by a solid vertical line. It is somewhat off from the observed peak position. Only, if we take into account the measured frequency shift of the $10_1^0 16_1^0$ two-photon transition, perfect agreement with the measured transition frequency is found.

The peak 158 cm^{-1} to the red of the $14_1^1 6_1^0$ band is assigned as the $14_0^1 15_1^0 6_1^0$ transition. It is due to a Duschinsky rotation (D) of the normal coordinate surfaces of the excited S_1 and the ground S_0 electronic state. This Duschinsky rotation was first concluded from intensity anomalies in the two-photon cold band and hot band spectrum of our previous work.[21] It can be described by

$$Q'_{14} = J_{14,14} \cdot Q''_{14} + J_{14,15} \cdot Q''_{15}, \tag{1}$$

where J_{ij} are the elements of the Duschinsky matrix J and the Q's are the respective normal coordinates. The ratio of the intensities of the $14_1^1 6_1^0$ and $14_0^1 15_1^0 6_1^0$ bands is given as

$$\frac{I(14_0^1 15_1^0 6_1^0)}{I(14_1^1 6_1^0)} = \frac{|J_{14,15}|^2}{|J_{14,14}|^2}. \tag{2}$$

From the theoretical work of Metz *et al.*[22] a value of 0.20 is predicted for the ratio while the results of Krogh–Jespersen *et al.*[23] would predict a value of 0.06. Due to the Fermi resonance between $14_1 6_1$ and $16_1 10_1 6_1$ discussed above, $I(14_1^1 6_1^0)$ has to be replaced by $I(14_1^1 6_1^0) + I(14_0^1 10_1^0 16_1^0 6_1^0)$ in Eq. (2). The evaluation of the experimental spectrum gives a value for $I(14_0^1 15_1^0 6_1^0)/[(I(14_1^1 6_1^0) + I(14_0^1 10_1^0 16_1^0 6_1^0)]$ of 0.16 ± 0.02 which seems to favor the calculation of Metz *et al.*[22] However, both the work of Metz *et al.*[22] and Krogh-Jespersen *et al.*[23] did not consider anharmonic effects, which have been proposed to be of great importance in this context.[24]

(iv) In summary, from this analysis it is clear that the observed perturbations result from a coupling in the ground state. We may conclude that there is no contribution to the 14^1, $J'_{K'} = 9_9$ state in C_6H_6 resulting from a coupling to background states in S_1. This state represents a pure zero-order state.

b. 21_{17} state in C_6D_6. In Fig. 5 the emission spectrum from the $J'_{K'} = 21_{17}$ state in the 14^1 vibronic state of C_6D_6 at a resolution of 50 cm^{-1} is shown. This rotational state was chosen as an unperturbed state since it corresponds to a strong rotational line which does not show any deviation from the theoretically expected position.

(i) The strong peaks are due to the $14_1^1 6_1^0 1_n^0$ progression. Most of the small peaks are analogous to the additional peaks in the emission spectrum from the 0^0 level of Ref. 19. In this way the $14_1^1 11_1^0 16_1^0$, $14_1^1 16_2^0$, $14_1^1 9_1^0$, $14_1^1 17_2^0$, and $14_1^1 7_1^0$ transitions can be assigned.

(ii) The remaining peaks at 37 295 and 37 590 cm^{-1}, respectively, need a more detailed discussion. First we have to check whether a Duschinsky rotation between modes ν_{14} and ν_{15} is also observed in C_6D_6 (such as C_6H_6). The transition $14_0^1 15_1^0 6_1^0$ would be expected at 38 450 cm^{-1}. Clearly no peak is seen at this position in the spectrum. This lack of Duschinsky rotation in C_6D_6 is in perfect agreement with the results of Metz *et al.*[22] and Krogh-Jespersen *et al.*[23] which would lead to a ratio $I(14_0^1 15_1^0 6_1^0)/I(14_1^1 6_1^0)$ of 0.009 and 0.0001, respectively. Even the $14_0^1 15_1^0 6_1^0 1_1^0$ band with an expected position at 37 505 cm^{-1} cannot explain the two peaks under discussion.

Next, known long-range anharmonic couplings or ground-state Fermi resonances (FG) have to be considered. This effect has been observed not only for C_6H_6 but also for C_6D_6 in our previous two-photon hot band measurements.[21] As a result, the peak at 37 295 cm^{-1} is assigned as the $14_0^1 10_1^0 16_1^0 6_1^0 1_1^0$ transition. It agrees well with the expected transition frequency.

Since the second peak at 37 590 cm^{-1} cannot be explained by either Duschinsky rotation or by anharmonic coupling in the ground state, the only explanation left is a coupling in the excited 14^1, $J'_{K'} = 21_{17}$ state. No deviation from the position of this state within the rotational contour is observed and therefore this coupling obviously does not re-

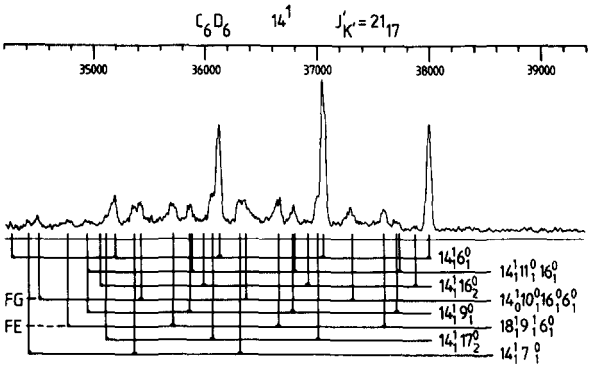

FIG. 5. Emission spectrum from the rotational state $J'_{K'} = 21_{17}$ of the 14^1 state of C_6D_6. Transitions resulting from long-range anharmonic couplings in the S_0 (S_1) state are labeled by FG (FE). 1^0_n must be added to every assignment. The origin of the band progression $14_0^1 10_1^0 16_1^0 6_1^0 1_n^0$ at 38 263 cm^{-1} is not marked.

sult in a rotational perturbation but rather might be an anharmonic coupling which shifts all rotational lines by the same amount. This would be the case, e.g., for a long-range Fermi resonance in the S_1 state. This hypothesis is further corroborated by additional emission spectra measured for the unperturbed 18_8, 21_6, and 24_{24} states. Even though the corresponding rotational lines reveal no deviation from the expected zero-order position, their emission spectra display the additional peak at 37 590 cm^{-1}. We checked all combination states with b_{2u} symmetry near the 14^1 (b_{2u}) state. Combination states with more than two vibrational quanta were not considered since their coupling matrix element would be too small to account for a long- range Fermi resonance. Within ± 100 cm^{-1} there is only one state of b_{2u} symmetry. This is the 18^19^1 state at about 1571 cm^{-1}. The frequency of this state is uncertain due to the badly known ν_9' frequency.[25] The transition frequency for the resulting $18_1^1 9_1^1 6_1^0$ transition is 37 591 cm^{-1} and in perfect agreement with the peak marked by FE in Fig. 5. A further confirmation of this assignment is given by comparison with C_6H_6. There, no excited state long-range Fermi resonance is observed. Due to the small deuterium isotope effect of the 14^1 state (C_6H_6:1571 cm^{-1}, C_6D_6:1567 cm^{-1}) on the one hand and the much stronger isotope effects in the 18^19^1 state, the energy difference of the 14^1 and the 18^19^1 state in C_6H_6 is 679 cm^{-1}. Furthermore, it is found for C_6H_6 that there are no other combination states of b_{2u} symmetry with two vibrational quanta within ± 100 cm^{-1} from the 14^1 state. The only background state which may give rise to a long-range Fermi resonance is present in C_6D_6 and is indeed detected and seen by the emission spectroscopy.

2. Rotationally resolved emission spectra

In the preceding subsection the vibrational character of the bands in the emission spectrum has been discussed. Now, we would like to identify the rotational structure of the emission bands. This is expected to be possible under the excitation conditions of the Doppler-free experiment leading to the excitation of defined single rotational states. For this reason the emission spectrum generally should consist of six lines resulting from $\Delta J = J' - J'' = -1, 0, +1$ (P,Q,R) and $\Delta K = K' - K'' = -1, +1$ (p,r) transitions for a perpendicular one-photon transition.[26] J' (J'') and K' (K'') are the rotational quantum numbers of the respective state in the S_1 (S_0) electronic state. Since the 14^1 state is nondegenerate ($l' = 0$, see below) and the final vibrational state in S_0 is degenerate, the respective rotational energies E'_{rot} in the excited state and E''_{rot} in the electronic ground state can be written as

$$E'_{rot} = B'[J'(J'+1) - K'^2/2], \tag{3}$$

$$E''_{rot} = B''[J''(J''+1) - K''^2/2] - B''l''\zeta''K''. \tag{4}$$

The implied assumption of $C = B/2$ is certainly valid for the accuracy of the emission spectra discussed. The rotational energy of the degenerate S_0 vibrational state [Eq. (4)] contains the additional Coriolis term which depends on the vibrational angular momentum component denoted by the l'' quantum number and the Coriolis coupling constant ζ''. According to Callomon *et al.*[26] only transitions with $\Delta l = l' - l'' = -l'' = \Delta K$ are allowed and therefore the change in rotational energy can be directly calculated for all six possible lines from Eqs. (3) and (4). The relative intensities of these lines are determined by the Hönl-London factors.[27] It is found, that within a good approximation the intensities of ${}^rR$ and ${}^pP$ lines are equal as well as for ${}^pR$ and ${}^rP$, and ${}^rQ$ and ${}^pQ$ lines, respectively. These results allow us to discuss two limiting cases of the influence of the rotational structure on the emission bands.

(i) If the rotational structure is not resolved, the position of the maximum of the band will coincide closely with the center of gravity of all six lines and may show a displacement from the rotationless position given by the vibronic frequencies alone. To calculate the center of gravity, the mentioned equality of the intensities of pairs of lines is used and the average of the change of rotational energy for each pair calculated:

$$1/2\cdot[\Delta E_{rot}({}^rR) + \Delta E_{rot}({}^pP)] = E'_{rot} - B''\cdot[J'(J'+1) - K'^2/2 + \zeta'' + \tfrac{1}{2}], \tag{5}$$

$$1/2\cdot[\Delta E_{rot}({}^pR) + \Delta E_{rot}({}^rP)] = E'_{rot} - B''\cdot[J'(J'+1) - K'^2/2 + \zeta'' + \tfrac{1}{2}], \tag{6}$$

$$1/2\cdot[\Delta E_{rot}({}^rQ) + \Delta E_{rot}({}^pQ)] = E'_{rot} - B''\cdot[J'(J'+1) - K'^2/2 + \zeta'' - \tfrac{1}{2}]. \tag{7}$$

The three expressions [Eqs. (5)–(7)] differ only by the term $B''(\zeta'' \pm \frac{1}{2})$ from the change in rotational energy of the ${}^qQ$ transition of the Doppler-free excitation. Since $|B''(\zeta'' \pm \frac{1}{2})| < 0.3$ cm^{-1}, a shift of the emission band from the rotationless origin by nearly the same amount as the displacement of the Doppler-free excitation line from the rotationless origin of the excitation band is expected. This displacement is nearly independent of ζ''.

(ii) For $J' = K'$ states only the ${}^rR$ and ${}^pP$ lines will carry significant intensity. Their splitting is given by

$$\Delta E_{rot}({}^rR) - \Delta E_{rot}({}^pP) = 2\cdot B''\cdot[2J' + 1 + K'(\zeta'' - 1)]. \tag{8}$$

This splitting depends linearly on $J' = K'$ and is strongly dependent on the value of ζ'' which differs for different vibrational states.

To test these predictions emission spectra were recorded with increased spectral resolution. In Fig. 6 the emission spectrum from the $J'_{K'} = 33_{33}$ state is shown under varying resolution of the dispersing monochromator. Under a resolution of $\Delta\nu = 20$ cm^{-1} the vibrational structure of the emission spectrum, which is only partially resolved under 50 cm^{-1} resolution, is completely resolved. It resembles the structure of the 9_9 state emission spectrum discussed in the preceding subsection. Thus, it is apparent that the 33_{33} state in 14^1 is unperturbed. The additional features in the emission spectrum result from Duschinsky rotation and Fermi resonances in the ground electronic state (see above).

We would like to emphasize that on the blue side of the $14_1^1 6_1^0$ transition a flat base line is observed with no noise on it. Apparently, there is no stray light present in the spectrum. Hence, it is concluded, that the irregular peak structure in the red part of the emission spectra represents a real struc-

ture rather than noise or stray light. This will be shown to be important for the discussion of the emission spectra of the $14^1 1^1$ state at higher excess energy.

At the bottom of Fig. 6 the two strong peaks $14_1^1 6_1^0$ and $14_1^1 6_1^0 1_1^0$ are shown under an increased resolution of $\Delta\nu = 5$ cm^{-1}. It is clearly seen that additional structure is resolved. Two peaks separated by 21 cm^{-1} are observed in the $14_1^1 6_1^0$ emission band and three peaks in the $14_1^1 6_1^0 1_1^0$ band. First, the splitting according to Eq. (8) was calculated for the $14_1^1 6_1^0$ band. The value of ζ'' for the $14_1 6_1$ state is not known, but it is expected to be nearly equal to $\zeta_6'' = 0.575$ known from previous work of Hollinger and Welsh.[28] The value of B'' was taken equal to the value of B_0'' determined by Pliva and Johns.[29] This leads to a calculated splitting of 20.1 cm^{-1}, in perfect agreement with the observed splitting. This means, that the two sharp peaks observed under 5 cm^{-1} resolution are indeed the transitions to the $J''_{K''} = 32_{32}$ and $J''_{K''} = 34_{34}$ rotational states.

The situation in the emission structure around 36 750 cm^{-1} is somewhat more complicated. There are three peaks observed, while only two (^rR and ^pP) lines would be expected. However, it has to be taken into account that there is a well-known Fermi resonance between the $6_1 1_1$ and the 8_1 state with a coupling matrix element of 9 cm^{-1}.[30] It can safely be assumed[17] that a similarly strong coupling exists between the states $14_1 6_1 1_1$ and $14_1 8_1$. We calculated the energies of the eigenstates in analogy to the Fermi dyad $6_1 1_1 / 8_1$.[31,32] There will be transitions to the $J''_{K''} = (34_{34})_a$, $(32_{32})_a$, $(34_{34})_b$, and $(32_{32})_b$ states with expected frequencies of 36 725, 36 744, 36 738, and 36 757 cm^{-1}, respectively. a (b) denotes the quasieigenstate at higher (lower) energy. The middle two lines are not resolved in the experimental spectrum, but give rise to the slightly broadened central feature. The observed distance of the other two lines from this central peak is in excellent agreement with the predicted one. These lines are again single rotational transitions.

The rotational splitting of the emission lines of the $14_1^1 6_1^0$ band was investigated for increasing J' in a systematic way. In Figs. 7 (a)–7(c) the resulting emission spectra are shown for upper states with $J' = K'$ and increasing J' ($J' = 9, 33, 75$). It is seen that the two strong emission lines resulting from the ^rR and ^pP transitions are separated for $J' > 33$ under the chosen experimental resolution of $\Delta\nu = 20$ cm^{-1}. The stick spectrum represents the calculated positions and intensities of the respective transitions. The arrow indicates the position of the rotationless transition. The expected small shift of the center of gravity of the lines with increasing rotational quantum number is clearly seen. This makes clear that even for a resolution not sufficient to resolve the rotational structure of the emission bands the position of their maximum relative to the pure vibrational transition frequency can be well understood. It is negligible for low

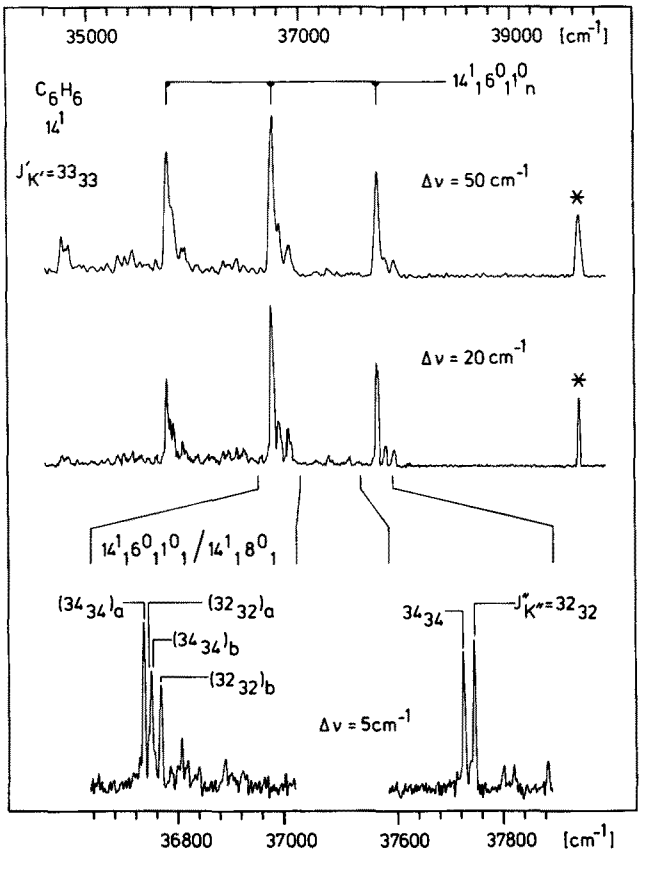

FIG. 6. Dispersed fluorescence from the $J'_{K'} = 33_{33}$ state in the 14^1 level of C_6H_6 measured under varying resolution of the dispersing spectrometer. The highly resolved spectrum at the bottom ($\Delta\nu = 5$ cm^{-1}) is shown on an extended frequency scale. An additional transition appears in the first progression member $14_1^1 6_1^0 1_1^0$ due to the Fermi resonance between the states $14_1 6_1 1_1$ and $14_1 8_1$.

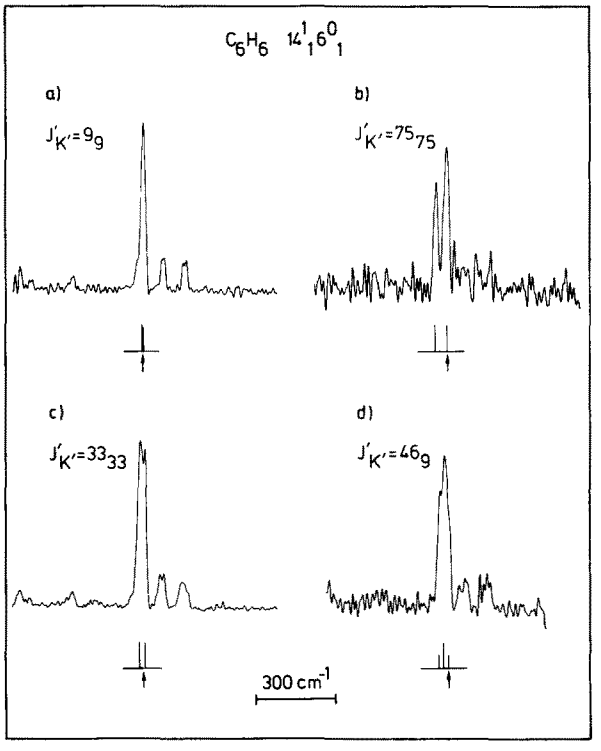

FIG. 7. Rotational structure of the $14_1^1 6_1^0$ emission bands from four different $J'_{K'}$ levels measured under a resolution of 20 cm^{-1}. The sticks below each spectrum represent the calculated individual rotational transitions. The calculated position of the rotationless origin in the emission band is indicated by the arrows.

rotational states like the $J'_{K'} = 9_9$ state. For excited states with K' strongly differing from J' the rotational structure cannot as easily be resolved, but instead is seen as a broadening of the observed band. This is demonstrated for $J'_{K'} = 46_9$ in Fig. 7(d).

3. Perturbed states

The analysis of rotational line positions in the 14^1_0 band of C_6H_6 led to the avoided crossings shown in Fig. 3. Emission spectra were measured for several perturbed states located near the crossing point of the term curves.

a. 21_{17} and 22_{17} states. In Fig. 8 the emission spectra of the $J'_{K'} = 18_8$ and the $(21_{17})_a$ state are shown for comparison. Both spectra were recorded at a resolution of 50 cm^{-1}. The corresponding two-photon excitation lines are only separated by less than 1 GHz (see the left-hand side of Fig. 8). From the analysis of the line positions the 18_8 state was found to be unperturbed, whereas the $(21_{17})_a$ line was found to be strongly perturbed and shifted by 0.42 GHz from the position calculated from the semirigid Hamiltonian with the constants of our recent work.[12,15] The unperturbed vs perturbed character of the 18_8 and the $(21_{17})_a$ state is fully corroborated by the emission spectra. The emission spectrum of the $J'_{K'} = 18_8$ state at the bottom of Fig. 8 is identical with the spectrum of the $J'_{K'} = 9_9$ state shown in Fig. 4. It is thus typical for an unperturbed state. The emission spectrum from the $(21_{17})_a$ state, however, shows additional features between the main $14^1_1 6^0_1 1^0_n$ progression bands which are not present in the spectrum of unperturbed states. It is interesting to note that emission spectra are seen to vary strongly within a few GHz of the rotational contour of the excitation spectrum. Emission spectra taken with Doppler-limited resolution of the excitation would be the superposition of differing emission spectra resulting from the various states simultaneously excited.

The $(21_{17})_a$ state is one eigenstate resulting from the coupling of the light 21_{17} state with a still unknown dark background state which is in accidental resonance. The other eigenstate $(21_{17})_b$ gives rise to a second line in the two-photon excitation spectrum which is located between the transitions leading to the unperturbed 19_{11} and 18_7 states (see the left-hand side of Figs. 8 and 9). The $(21_{17})_b$ line is somewhat smaller than the $(21_{17})_a$ line since it is not exactly at the crossing point of the term curves and contains more character of the dark background state than of the light 21_{17} state. This is nicely confirmed by the emission spectra of both components shown in Fig. 9. It is seen that in both spectra the additional band system appears which is characteristic of the dark state mixed in. In the emission spectrum of the $(21_{17})_b$ component the relative intensity of the additional band system is somewhat higher than in the $(21_{17})_a$ spectrum. This is in line with the increased dark character of this component.

The additional band system appearing in the emission spectra of the perturbed states is a fingerprint of the dark zero-order state mixed in. It is now used to identify the coupled dark background state. In Fig. 10 the emission spectrum of the $J'_{K'} = (22_{17})_a$ state is presented. As the 22_{17} state is further apart from the crossing point of the term curves than is the 21_{17} state (see Fig. 3), the $(22_{17})_a$ component contains an even stronger additional band system which is used for analysis of the dark state. All possible combination states with ungerade parity in the range 1571 ± 50 cm^{-1} were calculated in harmonic approximation. The range of ± 50 cm^{-1} was chosen since it is not expected that combination states which are apart more than 50 cm^{-1} in harmonic approximation for $J',K' = 0$ can come to exact resonance with the 14^1 light state for a J',K' value populated at room temperature. Ungerade parity was chosen since all possible low or high order coupling processes should couple only states of the same (ungerade) parity. In the chosen

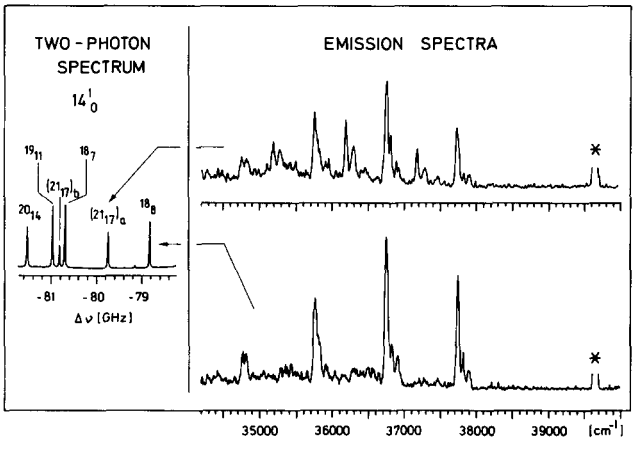

FIG. 8. Left-hand side: Part of the 14^1_0 two-photon excitation spectrum of C_6H_6. The upper rotational state of the corresponding transition is given on top of each line. Right-hand side: Comparison of the emission spectra from the perturbed state $J'_{K'} = (21_{17})_a$ and the unperturbed state $J'_{K'} = 18_8$ in the 14^1 state of C_6H_6. The corresponding transitions in the excitation spectrum are marked by arrows and are separated by less then 1 GHz. The additional band system in the upper spectrum is caused by the coupling of the light 14^1, 21_{17} state to a dark background state.

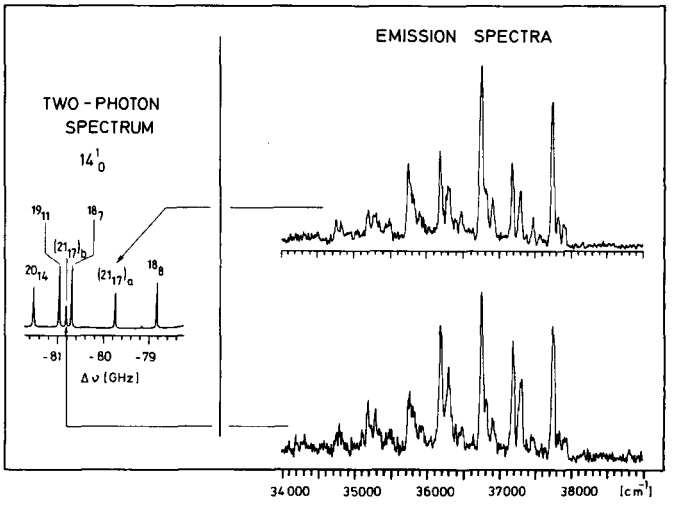

FIG. 9. Left-hand side: Part of the 14^1_0 two-photon excitation spectrum of C_6H_6. $(21_{17})_a$ and $(21_{17})_b$ indicate the two quasieigenstates resulting from the coupling of the light 21_{17} state to a dark rovibronic background state in S_1. Right-hand side: Emission spectra of the two quasieigenstates $(21_{17})_a$ and $(21_{17})_b$.

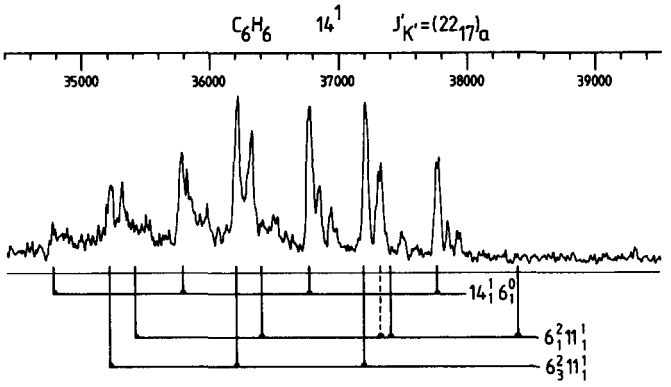

FIG. 10. Emission spectrum from the perturbed $J'_{K'} = (22_{17})_a$ state in the 14^1 level of C_6H_6. 1^0_n has to be added to every assignment. The solid marker lines indicate the calculated positions of the assigned transitions, the dashed marker indicates the observed position of the peak maximum of the $6^2{}_1 11^1{}_1 1^0{}_1$ transition. See the text for explanation of the difference.

interval 13 ungerade combination states are located. Only for one state the transition frequencies were found to coincide with the positions of the measured band systems. This is the $6^2 11^1$ state which contains a_{2u} and e_{2u} symmetry species and is located $-11\ \mathrm{cm}^{-1}$ from the 14^1 state in harmonic approximation. The two e_{2u} components $6^2(l = \pm 2)11^1$ are allowed to couple to the 14^1 (b_{2u}) state with a $\Delta K = \pm 1$ selection rule, like it is given, e.g., for perpendicular Coriolis coupling.[27] Two emission band systems $6^2_1 11^1_1 1^0_n$ and $6^2_3 11^1_1 1^0_n$ are expected for this state and indeed two band systems are observed in Fig. 10. The position and intensity of the two band systems, however, need a detailed discussion.

(i) $6^2_3 11^1_1$: The expected transition frequency coincides almost exactly with the stronger red peak in the emission spectrum.

(ii) $6^2_1 11^1_1$: The origin of this band system should be located at 38 362 cm^{-1}. No indication of a peak is seen there. Instead, the $6^2_1 11^1_1 1^0_1$ band forms the origin of this system. This is similar to the 6^2_1 system of Ref. 19 and may originate from the small Franck–Condon factor of the $6^2_1 11^1_1$ transition. In addition, there is a striking red shift of 70 cm^{-1} of the measured peak and the expected transition frequency (see dashed line in Fig. 10). A reasonable explanation for this red shift might be given by a Fermi resonance of the $6_1 11_1 1_1$ state with the $8_1 11_1$ state. This would be similar to the Fermi resonance of the $14_1 6_1 1_1$ and the $14_1 8_1$ state (see Fig. 6) and could lead to a repulsion of both states and the observed frequency shift. However, the frequency shift of the $6_1 11_1 1_1$ state is 70 cm^{-1} and therefore a factor of 6 larger than the frequency shift observed for the $14_1 6_1 1_1$ transition. The confirmation of large anharmonic couplings like this should be the subject of forthcoming theoretical investigations.

Another possible explanation of the peak assigned as $6^2_1 11^1_1 1^0_1$ can be deduced from very recent results of Page *et al.*[33] They deduced a value for the frequency of ν'_3 from IR–UV double resonance spectra of combination states which differs by 104 cm^{-1} from the value predicted by the calculation of Robey and Schlag.[34] This frequency value would place the state $3^1 16^1$ (e_{2u}) just 5 cm^{-1} below the 14^1 state. The frequency of the $3^1_1 16^1_1 6^0_1$ emission band would perfectly fit our observed peak. However, assuming solely a coupling to the $3^1 16^1$ state the appearance of the second stronger peak to the blue, which can nicely be explained by the assignment $6^2_3 11^1_1$ would not be understandable. A hypothetical remedy for this problem would be a Fermi resonance of $6^2 11^1$ and $3^1 16^1$ which in turn couples by higher order rotation–vibration coupling to 14^1 and then gives rise to the observed emission pattern.

b. 46_9 and 35_{15} states in C_6H_6. In Fig. 11 the emission spectra of the two eigenstates $J'_{K'} = (46_9)_a$ and $(35_{15})_a$ are presented. The residuals of Fig. 3 indicate that both state positions are shifted from the position of the zero-order states and thus both states are coupled to dark background states. It is seen that again additional band systems appear in the emission spectrum which are identical to those shown above in Fig. 10. It is thus clear that these perturbations are caused by the same background states ($6^2 11^1$ and/or $3^1 16^1$). Obviously several crossings of the term curves of these states and the 14^1 state occur for different J', K' levels.

c. 25_9 state. For the $K' = 9$ states a second crossing is observed which is located at a relatively low J level ($21 < J' < 33$; see Fig. 3). The emission spectrum of the $(25_9)_a$ component is shown in Fig. 12. In addition to the band system resulting from the light 14^1 state another system is recognized which differs, however, from the already known additional band system in Figs. 10 and 11. The additional peak at 36 816 cm^{-1} is not far from the $14^1_1 6^0_1 1^0_1$ transition. It can be readily and unambiguously assigned as the $5^1_1 10^1_1 16^1_1 6^0_1$ transition. This transition is due to the coupling of the 14^1 state to the $5^1 10^1 16^1$ state which is one of the 13 ungerade combination states within the interval 1571 ± 50 cm^{-1}. It is located $-7\ \mathrm{cm}^{-1}$ from the 14^1 state in harmonic approximation and contains vibrational angular momentum components of a_{1u}, a_{2u}, and e_{2u} symmetry. Since no quantum of ν_6 is part of the combination state only one emission band system is expected and indeed observed.

d. 29_{29} state in C_6D_6. The analysis of rotational line positions in the 14^1_0 band of C_6D_6 shows that the 29_{29} line is

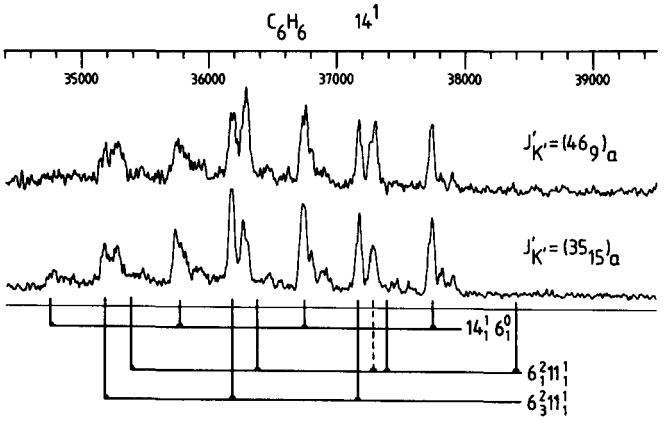

FIG. 11. Emission spectra from the perturbed $J'_{K'} = (46_9)_a$ and $J'_{K'} = (35_{15})_a$ rotational states in the 14^1 state of C_6H_6. 1^0_n has to be added to every assignment. The solid marker lines indicate the calculated positions of the assigned transitions.

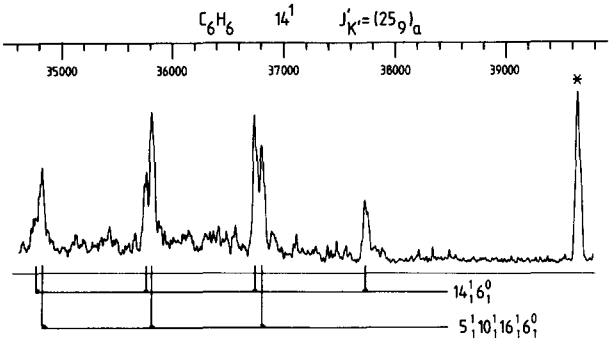

FIG. 12. Emission spectrum from the perturbed state $J'_{K'} = (25_9)_a$ in the 14^1 level of C_6H_6. 1^0_n has to be added to every assignment.

shifted by 0.5 GHz from the zero-order position. This is a strong indication for the perturbed character of this line. For confirmation the emission spectrum from the $(29_{29})_a$ state was measured and is displayed in Fig. 13. A comparison with the emission spectrum from the unperturbed 21_{17} state (see Fig. 5) shows that the spectrum in Fig. 13 is contaminated by two additional bands with peak positions at 37 499 and 37 295 cm^{-1}. For identification the procedure described in Sec. I was applied. Due to its lower vibrational frequencies the density of states in C_6D_6 is by a factor of 3–4 higher than in C_6H_6 and 47 ungerade states are located in the chosen frequency interval 1567 ± 50 cm^{-1}. However, in this range there exists only one state which leads to emission bands whose transition frequencies agree with the experimental ones within the experimental accuracy of ± 10 cm^{-1}. This is the $4^1 6^1 18^1$ state which is located at 1568 cm^{-1} in harmonic approximation. The two additional band systems are assigned as the $4^1_1 18^1_1 6^1_0$ and the $4^1_1 18^1_1 6^1_2$ transitions. The appearance of two additional band systems caused by one coupled state is due to the ν_6 quantum present in the coupled dark $4^1 18^1 6^1$ state.

4. Summary for the 14^1 state

From emission spectroscopy it is found that the 14^1 state in C_6H_6 is not perturbed by *long-range* Fermi resonances. As a consequence more than 90% of the rovibronic states represent pure zero-order states in S_1. However, about 10% of the rovibronic states are perturbed by *short-range* coupling to dark background states in S_1. Emission spectroscopy of selected perturbed states has enabled us to identify some of the coupled states. It is interesting to note that in every case investigated the coupled state is composed of three vibrational quanta and includes an e_{2u} symmetry component. From this and the rotationally dependent coupling matrix element we conclude that the couplings are produced by H_{42} resonances[35] due to a higher order vibration-rotation coupling. The mixing is quite effective. For states at the crossing point a 50:50 mixture of the light and the dark states is evident from the emission spectra.

The situation is somewhat different in C_6D_6. Even for rotational lines which do not show a shift from the expected position emission spectroscopy reveals a contamination by a combination state of two vibrational quanta. As this contamination is present for many nonshifted lines it is concluded that long-range anharmonic coupling is responsible for the mixing and leads to an homogenous shift of all rotational lines. This is not detected in the analysis of the rotational line positions. Due to the isotopic shift of the vibrational frequencies the long-range anharmonic coupling to this state is not present in C_6H_6. In addition, from emission spectroscopy we learn that vibration–rotation coupling by H_{42} resonances causes rotational perturbations in C_6D_6. These *short-range* couplings lead to a much stronger and more effective mixing of the light and the dark zero-order states than the *long-range* Fermi resonances. This is clearly demonstrated by the appearance of strong additional bands in the emission spectra.

C. Emission spectra from single rotational states in the $14^1 1^1$ state

1. Unperturbed states

a. 23_{23} state in C_6H_6. In Fig. 14 the emission spectrum from the 14^1, $J'_{K'} = 23_{23}$ rotational state is shown. The corresponding rotational line in the Q branch of the $14^1_0 1^1_0$ band

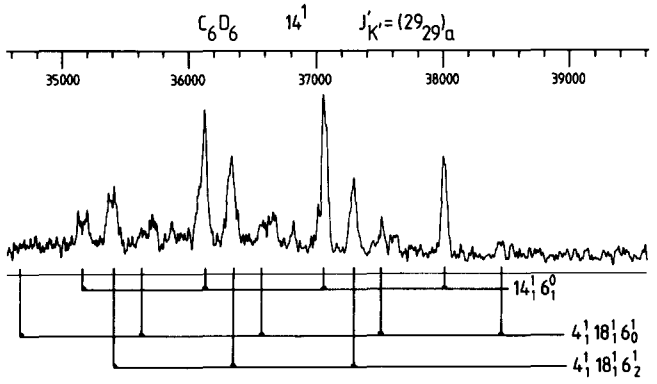

FIG. 13. Dispersed fluorescence from the perturbed state $J'_{K'} = (29_{29})_a$ in the 14^1 state of C_6D_6. 1^0_n has to be added to every assignment.

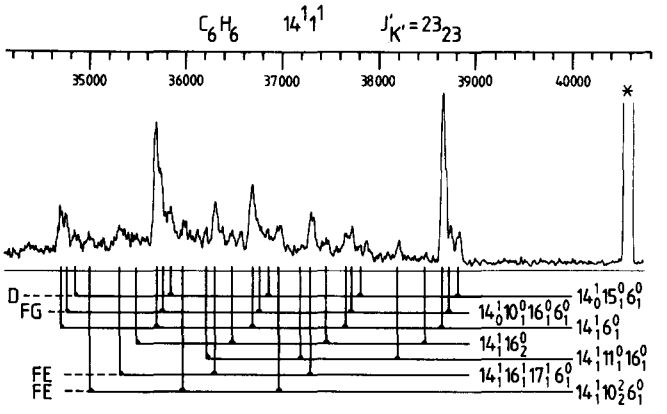

FIG. 14. Dispersed fluorescence from the rotational state $J'_{K'} = 23_{23}$ in the $14^1 1^1$ vibronic state of C_6H_6. D indicates transition due to a Duschinsky rotation of the normal coordinate surfaces in the excited (S_1) vs ground electronic state (S_0). FG (FE) is a long-range Fermi resonance in the ground (excited) electronic state. 1^0_n has to be added to the assignments which are marked by FE, otherwise 1^1_n.

was not found to be shifted from the zero-order position within the rotational contour. Hence, this line does not display a rotational perturbation. Most of the features in Fig. 14 are identical with those of the emission spectrum from unperturbed rotational states in the 14^1 state. In addition, two band systems appear with peaks at 37 318 and 36 974 cm^{-1}, respectively. These band systems are also found for other unperturbed states (e.g., 22_{17}). Thus, it is argued that they are produced by a long-range Fermi resonance in the excited state. It has been shown in our previous work[21] that the $14^1 1^1$ state in C_6H_6 is coupled to the $14^1 16^1 17^1$ state by long range anharmonic coupling. This gives rise to a "shadow" progression in the two-photon excitation spectrum. A similar situation arises for C_6D_6, where long-range anharmonic interaction of the $14^1 1^1$ state with the $14^1 10^2$ state occurs. The energy difference of the $14^1 1^1$ state and the $14^1 16^1 17^1$ state is 32 (89) cm^{-1} and the $14^1 10^2$ state 237 (29) cm^{-1} for C_6H_6 (C_6D_6), respectively.

Both the Fermi resonances with the $14^1 16^1 17^1$ and the $14^1 10^2$ state are detected in the emission spectrum of C_6H_6. However, it is surprising that the coupling to the $14^1 10^2$ state, which is 237 cm^{-1} apart, can lead to an observable contamination in the emission spectrum. The emission spectrum shown in Fig. 14 is a direct corroboration of our previous assignment of the "shadow" progressions and demonstrates its sensitivity for detection of mixing of states. The Franck-Condon factors of the $14_1^1 6_1^0 1_n^1$ progression band are found to be different from those of the $14_1^1 6_1^0 1_n^0$ progression shown in Fig. 4. This is similar to what has been found by Knight *et al.*[19] for the $6_0^1 1_n^0$ and $6_0^1 1_n^1$ progression bands. By contrast, the Franck–Condon factors of the band system resulting from the coupled $14^1 16^1 17^1$ state resemble those of the $14_1^1 6_1^0 1_n^0$ band system in Fig. 4, since there is no ν_1 vibration present in the excited state.

In Fig. 14 a background in the emission spectrum is observed, which increases for decreasing transition frequencies and displays a maximum at 36 200 cm^{-1}. Its integrated area is 0.8 of the integrated area of all sharp peaks in the emission spectrum. We would like to emphasize again that the emission spectrum in Fig. 14 was measured after excitation of a single defined two-photon line, i.e., of a defined rovibronic state of the molecule. Thus, the background cannot be the result of a hot band congestion or of an incoherent simultaneous excitation of several levels whose emission bands may overlap. The origin of the background in our measurements will be discussed in more detail below.

b. 18_{18} state in C_6D_6. In Fig. 15 the emission spectrum from the 18_{18} state in the $14^1 1^1$ vibronic state of C_6D_6 is shown. Recently, we found that the $14_0^1 1_0^1$ band in C_6D_6 is strongly perturbed.[15] This was demonstrated by the statistical analysis of line intensities. Only the $J' = K'$ lines, which are the strongest lines in the Q branch of the $14_0^1 1_0^1$ band, could be assigned since their position is not affected by a coupling process. Most of the features in the spectrum of Fig. 15 are identical to those shown in Fig. 5 for the 14^1 state. The additional two band systems are attributed to long-range Fermi resonances to the $14^1 10^2$ and $14^1 16^1 17^1$ states which are displaced by 29 and 89 cm^{-1}, respectively from the $14^1 1^1$ state. The anharmonic coupling to the $14^1 10^2$ state was assumed to lead to the "shadow" progression bands in the two-photon excitation spectrum in our previous work.[21]

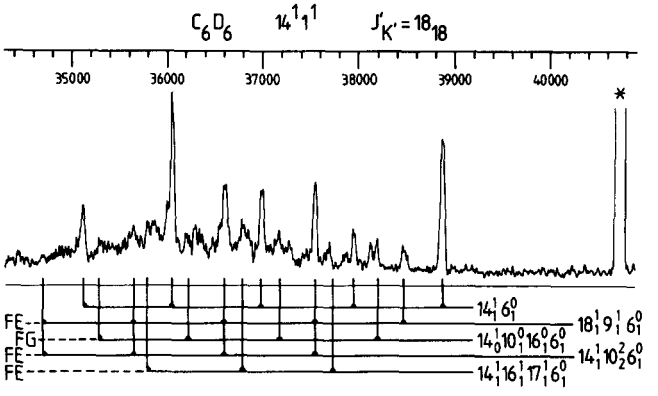

FIG. 15. Dispersed fluorescence from the rotational state $J'_{K'} = 18_{18}$ in the $14^1 1^1$ vibronic state of C_6D_6. FG (FE) is a long-range Fermi resonance in the ground (excited) electronic state. 1_n^0 has to be added to the assignments $14_1^1 10_2^2 6_1^0$ and $14_1^1 16_1^1 17_1^1 6_1^0$, otherwise 1_n^1.

From the emission spectra of the $14^1 1^1$ states in C_6H_6 and C_6D_6 it is seen that both states are only weakly contaminated by long-range coupling. In both emission spectra (Figs. 14 and 15) there is a background, which is peaked around 36 000 cm^{-1}.

2. Perturbed states in C_6H_6 and C_6D_6

In our recent work[12] we analyzed a rotational perturbation in the Doppler-free rotational line spectrum of the $14_0^1 1_0^1$ band of C_6H_6. Nonzero residuals were found for $K' = 3$ lines in the range $10 < J' < 23$ with an approximate crossing point of the term curves at $J' = 16$. The emission spectrum from the $(16_3)_b$ eigenstate is shown in Fig. 16. Comparison of Fig. 16 with the emission spectrum from an unperturbed state in Fig. 14 reveals that the emission spectrum is contaminated by a strong sharp additional band system, marked by X, with its origin at 38 217 cm^{-1}. In order to analyze the coupled dark state which gives rise to the addi-

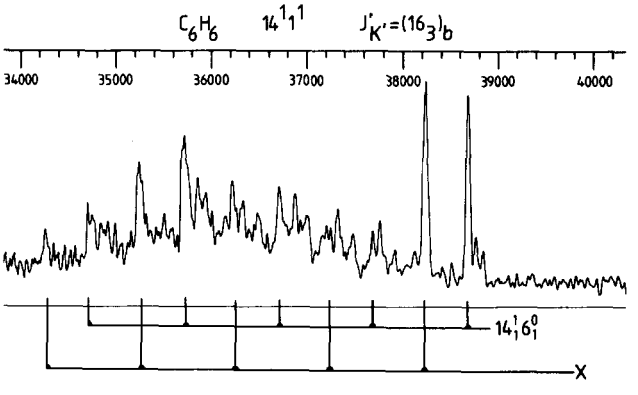

FIG. 16. Emission spectrum of the perturbed rotational state $J'_{K'} = (16_3)_b$ in the $14^1 1^1$ state of $C_6H_6 1_n^1$ has to be added to the assignment. X indicates an additional band system which arises due to a coupling of the light state to a dark background state, probably a rotational state of the $3^1 16^1 1^1$ vibronic state (for explanation, see the text).

tional band system all harmonic combination states in the vicinity of the $14^1 1^1$ state together with the resulting emission frequencies were considered. The excess energy of the $14^1 1^1$ state is 2493 cm^{-1}. As a consequence of the high excess energy of this state the density of states is now 18 $1/cm^{-1}$. 129 ungerade combination states were found in the frequency interval 2493 $\pm$ 50 cm^{-1} according to the harmonic calculation.[20] No agreement of any of the resulting transition frequencies with the measured ones was found within the experimental accuracy. Hence, we are not able to unambiguously identify the coupled state on the basis of the used frequencies.[20] There are, however, several arguments which lead to an approximative description of the coupled state.

(i) The band origin is close to the origin of the $14_1^1 6_1^0 1_n^1$ progression band. From this it is clear that the combination state cannot include a great number of vibrational quanta. A great number of vibrational quanta would lead to a strong red shift of the origin as vibrational frequencies generally increase in the ground state. Here, it has been assumed that Franck–Condon factors are largest for emission to a final state with equal number of vibrational quanta.

(ii) The Franck–Condon factors for the X band system are identical to those of the $14_1^1 1_n^1 6_1^0$ band system and thus typical for emission from an excited state including one quantum of ν_1'. This conclusion is in complete agreement with the small red shift observed for the additional band system. Here, the Franck–Condon factor for emission is largest if the ν_1 quantum is not excited in the ground state. This leads to a high transition frequency which is indeed observed in the experiment. If both the light $14^1 1^1$ and the still unknown dark X^1 state include one quantum of ν_1, the X^1 state should also be a candidate for short-range coupling in the 14^1 state.

These arguments lead us back to the investigation of the dark state perturbing the 14^1 vibronic state. We mentioned at that point, that the recent determination of the frequency of ν_3' (Ref. 33) would place the $3^1 16^1$ state in close resonance with the 14^1 state and therefore it follows, that also the $3^1 16^1 1^1$ state would be in close resonance with the $14^1 1^1$ state. The emission band $3_1^1 16_1^1 6_1^0 1_0^1$ would be expected consequently at 38 219 cm^{-1} and therewith in perfect agreement with the observed band position (38 217 cm^{-1}). The $3^1 16^1 1^1$ state would meet all the criteria deduced above and there is no problem of an additional band system to be explained like in the case of the perturbed 14^1 states. It remains, however, to be seen, whether the new determination of the ν_3' frequency[33] stands up to further consistency tests.

Even though the unambiguous assignment of the coupled dark state is not straightforward for the $14^1 1^1$ state at 2493 cm^{-1} excess energy it is without doubt that there still exists a highly selective coupling at this high excess energy with high density of background states (18 $1/cm^{-1}$). The emission spectrum displays distinct features which can only be explained by a coupling between pairs of states. In addition to this selective coupling the spectrum in Fig. 16 displays a broad background with maximum at 36 200 cm^{-1}. The integrated area of this background is a factor of 1.05 of the integrated area of all sharp peaks in the spectrum. Before we shall discuss the origin of this background we would like

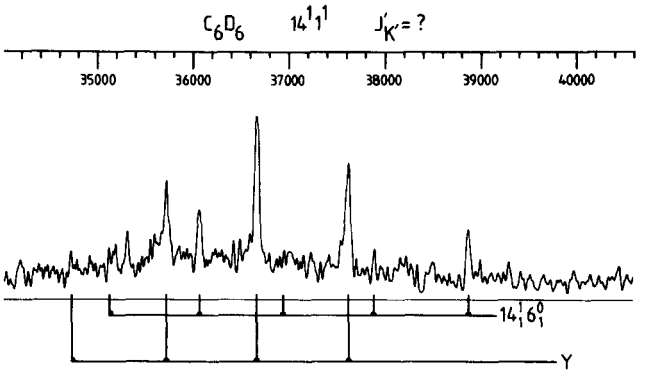

FIG. 17. Emission spectrum of an unidentified rotational state in the $14^1 1^1$ state of C_6D_6. 1_n^1 has to be added to the assignment. The additional band system labeled by Y is produced by a coupling to an unknown dark background state.

to briefly report on results for C_6D_6.

In Fig. 17 the emission spectrum from a perturbed rotational state in the $14^1 1^1$ state of C_6D_6 is shown. This rotational state cannot be assigned because of the perturbed character of the rotational line structure of the $14_0^1 1_0^1$ band.[15] It is located at $-$ 44 GHz to the red of the rotationless origin. In addition to the $14_1^1 6_1^0 1_n^1$ band system due to the light $14^1 1^1$ character of this state another even stronger band system (Y) appears. Because of the high density of background states (60 $1/cm^{-1}$) it is not possible to unambiguously identify the coupled background state on the basis of the observed transition frequency. We measured the emission spectra from four other perturbed states which are located between 40 and 60 GHz to the red of the rotationless origin of the $14_0^1 1_0^1$ band. All emission spectra display the same additional bands (Y), however, with varying intensity. From this we may conclude that most of the rotational states in the $14^1 1^1$ state are perturbed by selective coupling to only one dark background state. The degree of coupling varies strongly from one rotational state to another and results in the strongly perturbed character of the rotational contour of this band. Most likely, this random coupling is responsible for the line intensity distribution of this band discussed in our recent work.[15]

The origin of the additional band system (Y) is about 1200 cm^{-1} to the red of the $14_1^1 6_1^0 1_0^1$ origin. This is different from the situation in the $14^1 1^1$ state of C_6H_6 (see Fig. 16) where the red shift is only about 450 cm^{-1}. In addition, the Franck–Condon behavior of the progressions of the Y band differs from that of the X band in C_6H_6. From both points we conclude that the coupled dark background state does not contain a quantum of the ν_1 vibration. For this reason the observed resonance is present only in the $14^1 1^1$ state but does not exist in the 14^1 fundamental state. This explains why the $14_0^1 1_0^1$ band in C_6D_6 is so strongly perturbed, whereas the 14_0^1 band is not. A possible candidate for the dark background state which perturbs so efficiently the $14_0^1 1_0^1$ band in C_6D_6 might be the 15^3 state of b_{2u} symmetry which is located only 4 cm^{-1} from the $14^1 1^1$ state in the harmonic approximation. The transition frequency of the $15_3^3 6_1^0$ band is 37 680 cm^{-1}. This is shifted by 60 cm^{-1} from the band in the emission spectrum (see Fig. 17). This discrepancy is not the un-

certainty of the experiment, so that only a tentative assignment can be given. The shift might be produced by anharmonicities.

3. The origin of the background

In the preceding subsection we have shown that the intrastate coupling is still highly selective in C_6H_6 and C_6D_6 at an excess energy of more than 2400 cm^{-1} with a density of states of 18 and 60 $1/cm^{-1}$, respectively. However, in addition to this selective coupling a background was observed, which appears to be smaller in the emission spectrum from the 14^1 state. The question is whether this background is produced by frequent intrastate coupling. In previous work the appearance of a background was interpreted as an indication for the presence of IVR.[1-3] In this experiment, which guarantees precise excitation conditions we have shown, that for an excess energy, which leads to the appearance of a background at the same time selective coupling for distinct states is observed.

(i) It is not straightforward to interpret the background in our emission spectra as the result of a coupling process in the statistical limit or at least to many states due to the following arguments. The spectral resolution in the emission spectra from the $14^1 1^1$ state is better than 50 cm^{-1}. In order to produce an unresolved broad background the different emission bands should be located at an average distance of 50 cm^{-1}. Every emission band would be expected to display a progression band every 993 cm^{-1} (946 cm^{-1}) in C_6H_6 (C_6D_6). From that, it is clear, that at least 20 emission bands should be located within 993 cm^{-1} and thus a coupling to more than 20 states should occur. Frequent couplings like this cannot be explained on the basis of the low density of background states which is 18 $1/cm^{-1}$ for C_6H_6 and 60 $1/cm^{-1}$ for C_6D_6 and the small coupling matrix elements expected for the higher order coupling processes which would be responsible for the frequent couplings. We have explicitly shown by a detailed spectral analysis for C_6H_6 that couplings with coupling matrix elements around 1 GHz still lead to selective coupling between pairs of states. Hence, for the low density of states, it is very unlikely, that a defined rovibrational state can be coupled to 20 states if at the same time this state is selectively coupled to a single dark state by a coupling matrix element of some GHz. This is further corroborated by the high-resolution Doppler-free two-photon excitation spectra presented in our previous work.[12,15] Coupling to many states would result in additional lines in the excitation spectrum as the light character of the $14^1 1^1$ state would be distributed on many resulting eigenstates. No additional lines are observed in the Doppler-free two-photon excitation spectrum even for the very high resolution in the order of 10 MHz. In addition, no line broadening in excess of 5 MHz was found. These experimental results would only permit a frequent coupling with coupling matrix elements of less than 10 MHz. It is, however, not clear, how frequent couplings with matrix elements in the order of 10 MHz can occur if the average spacing of dark background states is more than 1 GHz. From this it is very unlikely that the observed background is due to IVR in the excited state.

(ii) In order to explain the origin of the background another effect has to be taken into account. This is emission from states originally not excited by the laser light but populated by collisions. After several collisions, emission from the thermalized S_1 state occurs. In a separate experiment we have checked the amount of fluorescence after collisional deactivation and from the thermalized S_1 level. It was found that the maximum of the emission from the thermalized S_1 level is located around 36 000 cm^{-1} in C_6H_6. This corresponds to the $6_1^0 1_1^0$ band and several sequence bands. It was further found that for a pressure of 2.5 Torr the integrated emission from the originally populated $14^1, J'_{K'}$, level (resonant emission) is 0.2 of the integrated area of the nonresonant emission after collisional depopulation of the originally excited level. The measurements of this work have been performed at a pressure of about 0.25 Torr. For this pressure the ratio of resonant fluorescence and nonresonant emission is estimated to be 2.6. This is in very good agreement with the experimental result shown in Fig. 4. There, the integrated area of the sharp resonant emission is found to be 2.6 of the area of the background from nonresonant emission.

The situation is somewhat different for the $14^1 1^1, J'_{K'}$, levels. Firstly, the quantum yield for fluorescence is decreased by 40% (Ref. 36) due to the higher excess energy, whereas that of the states populated by collisions at lower excess energy may not. Secondly, additional bands due to long-range coupling appear, which may overlap and contribute to the unresolved background around 36 000 cm^{-1}. As a consequence, relative intensity of the nonresonant emission increases. Hence, the increase of a factor of 2 in the unresolved background observed for the $14^1 1^1$ state as compared to the 14^1 state can be qualitatively explained by nonresonant emission. In summary, it seems more likely that the observed background in the emission spectra from the $14^1 1^1$ level results from nonresonant emission rather than from an IVR process in the excited state.

IV. SUMMARY AND CONCLUSION

In this work we presented emission spectra from several defined rovibronic states at different excess energies in benzene. The combination of Doppler-free two-photon absorption and a long-term frequency stabilization of the exciting single-mode dye laser enabled us to selectively excite defined quantum states and to measure the dispersed emission spectra from these states. Emission spectra reveal a great number of detailed results on Duschinsky rotation and Fermi resonances in the ground state.

For a low excess energy of 1571 cm^{-1} it is seen that most of the rotational states in the 14^1 vibronic state of C_6H_6 are "pure" states, i.e., no additional vibrational character due to a long-range anharmonic coupling is mixed in. Some of the investigated states have been identified as perturbed ones from the analysis of the line positions in the Doppler-free two-photon excitation spectrum. Emission spectra from these states clearly demonstrate that additional vibrational character from a dark background state is mixed in by selective coupling between pairs of states and leads to localized perturbations of the rovibronic band by dark states. The coupled background states were identified on the basis of the

typical emission bands. They are combination states including three vibrational quanta. The mechanism responsible for the mixing of states is a H_{42} resonance due to high-order rotation–vibration interaction. For states near the crossing point of the term curves a very efficient (50:50) mixing of the light and the dark state is found. Basically the same result is present in the 14^1 state in C_6D_6 even though there is a negligible contamination ($< 10\%$) of all rotational states by a long-range anharmonic coupling. In addition, very efficient mixing is detected for several states due to short-range high-order rotation–vibration interaction.

In the $14^1 1^1$ vibronic state at a higher excess energy of 2493 cm^{-1} in C_6H_6 and 2445 cm^{-1} in C_6D_6 all rotational states are moderately contaminated due to long-range anharmonic interaction. The density of states at this excess energy has increased to 18 $1/cm^{-1}$ and 60 $1/cm^{-1}$ in C_6H_6 and C_6D_6, respectively. For this reason it might be argued that frequent couplings to several background states can occur. Emission spectra clearly demonstrate that even for a total density of states of 60 $1/cm^{-1}$ the coupling is very selective and occurs between pairs of states. This is deduced from the appearance of sharp additional peaks in the emission spectrum after excitation of rotational lines which have been found to be strongly perturbed in the Doppler-free two-photon excitation spectrum.[12,15] Even under sharp excitation conditions and only selective couplings present some broad band background is observed in the emission spectra. This simultaneously observed background is believed to be due to nonresonant fluorescence from states populated by collisions rather than to a coupling of many states or to a coupling in the statistical limit. With this result in mind it appears to be questionable, whether a background appearing in emission spectra can always be interpreted as caused by IVR.

The spectroscopic results of this work yield basic information for the understanding of the intramolecular-vibrational redistribution process (IVR).

(i) Short-range couplings lead to a more effective mixing of light and dark states in S_1 than is observed for long-range Fermi resonances.

(ii) High-order rotation–vibration interaction is an important mechanism for the mixing of states.

(iii) Even for densities of states as high as 60 $1/cm^{-1}$ coupling is found to be very selective and leads to the interaction of pairs of states.

In view of these results it is concluded that dynamic IVR due to coupling within a single electronic potential surface is possible only for much higher density of states present only at even higher excess energies. In S_1 benzene the sufficient density of states would be reached not below 4000 cm^{-1} of vibrational excess energy. This conclusion is in good agreement with recent results from chemical timing experiments of Longfellow *et al.*[37] and decay time measurements in our group.[38] From the chemical timing experiments an unexpectedly low density of coupled states was found for the $6^1 1^2$ and $6^1 1^3$ states of C_6H_6 at an excess energy of 2370 cm^{-1} and 3290 cm^{-1}, respectively. Decay times of various rotational states in the $14^1 1^2$ vibronic state were found to vary strongly with the rotational quantum number J. This was explained by a selective coupling to a single, strongly broadened vibronic background state in S_1 rather than by a coupling to many vibronic states in S_1.

ACKNOWLEDGMENTS

The authors are indebted to Professor E. W. Schlag for his continuous interest in the progress of this work and stimulating discussions. They thank F. Giesemann for his assistance during the early part of the experiment. Discussions with Professor C. S. Parmenter have been most encouraging. Financial support from the Deutsche Forschungsgemeinschaft and from the Fonds der Chemischen Industrie is gratefully acknowledged.

[1] C. S. Parmenter and M. W. Schuyler, J. Chem. Phys. **52**, 5366 (1970).
[2] H. F. Kemper and M. Stockburger, J. Chem. Phys. **53**, 268 (1970).
[3] R. A. Coveleskie, D. A. Dolson, and C. S. Parmenter, J. Chem. Phys. **72**, 5774 (1980).
[4] J. M. Blondeau and M. Stockburger, Ber. Bunsenges. Phys. Chem. **75**, 450 (1971).
[5] R. E. Smalley, J. Phys. Chem. **86**, 3504 (1982).
[6] D. V. O'Connor, M. Simutani, Y. Takagi, N. Nakashima, K. Kamogawa, Y. Udugawa, and K. Yoshihara, Chem. Phys. **93**, 373 (1985).
[7] T. A. Stephenson, P. Radloff, and S. Rice, J. Chem. Phys. **81**, 1060 (1984).
[8] A. E. W. Knight, Ber. Bunsenges. Phys. Chem. **92**, 337 (1988).
[9] E. Riedle, H. J. Neusser, and E. W. Schlag, J. Chem. Phys. **75**, 4231 (1981).
[10] E. Riedle and H. J. Neusser, J. Chem. Phys. **80**, 4686 (1984).
[11] U. Schubert, E. Riedle, and H. J. Neusser, J. Chem. Phys. **84**, 5326 (1986).
[12] E. Riedle, H. Stepp, and H. J. Neusser, Chem. Phys. Lett. **110**, 452 (1984).
[13] T. W. Hänsch and B. Coulliaud, Opt. Commun. **35**, 441 (1980).
[14] F. Giesemann and E. Riedle (unpublished).
[15] H. Sieber, E. Riedle, H. J. Neusser, J. Chem. Phys. **89**, 4620 (1988).
[16] E. Riedle and H. J. Neusser, Comments At. Mol. Phys. **19**, 331 (1987).
[17] A. E. W. Knight and C. S. Parmenter, Chem. Phys. Lett. **43**, 399 (1976).
[18] C. S. Parmenter, K. Y. Tang, and R. Ware, Chem. Phys. **17**, 359 (1976).
[19] A. E. W. Knight, C. S. Parmenter, and M. W. Schuyler, J. Am. Chem. Soc. **97**, 1993, 2005 (1975).
[20] The frequencies used for harmonic level calculations are as tabulated by Stephenson *et al.* (Ref. 7) C_6H_6 and supplemented by the calculated frequencies of Robey and Schlag (Ref. 34) where no measured ones were known. For C_6D_6 the values tabulated by Ziegler and Hudson (Ref. 25) were used.
[21] L. Wunsch, F. Metz, H. J. Neusser, and E. W. Schlag J. Chem. Phys. **66**, 386 (1977).
[22] F. Metz, M. J. Robey, E. W. Schlag, and F. Dörr, Chem. Phys. Lett **51**, 8 (1977).
[23] K. Krogh-Jespersen, R. P. Rava, and L. Goodmann, J. Phys. Chem. **88**, 5503 (1984).
[24] L. Goodman, J. M. Berman, and A. G. Ozkabak, J. Chem. Phys. **90**, 2544 (1989).
[25] L. D. Ziegler and B. S. Houdson, in *Excited States*, edited by E. C. Lim (Academic, New York, 1982).
[26] J. H. Callomon, T. M. Dunn, and I. M. Mills, Philos. Trans. R. Soc. London, Ser. A **259**, 449 (1966).
[27] G. Herzberg, *Molecular Spectra and Molecular Structure* (Van Nostrand, Princeton, 1959), Vol. III, p. 226.
[28] A. B. Hollinger and H. L. Welsh, Can. J. Phys. **56**, 1513 (1978).
[29] J. Pliva and J. W. C. Johns, Can. J. Phys. **61**, 269 (1983).
[30] W. R. Augus, C. R. Bailey, J. B. Hale, C. K. Ingold, A. H. Leckie, C. G. Raisin, J. W. Thompson, and C. L. Wilson, J. Chem. Soc. **1936**, 931; S. Brodersen and A. Langseth, Mat. Fys. Skr. Dan. Vid. Selsk. **1**, 1 (1956).
[31] P. Esherick, A. Owyoung, and J. Pliva, J. Chem. Phys. **83**, 3311 (1985).

[32]J. Pliva, P. Esherick, and A. Owyoung, J. Mol. Spectrosc. **125**, 393 (1987).
[33]R. H. Page, Y. R. Shen, and Y. T. Lee, J. Chem. Phys. **88**, 5362 (1988).
[34]M. J. Robey and E. W. Schlag, J. Chem. Phys. **67**, 2775 (1977).
[35]M. R. Aliev and J. K. G. Watson, in *Molecular Spectroscopy: Modern Research*, edited by K. N. Rao (Academic, New York, 1985).
[36]L. Wunsch, H. J. Neusser, and E. W. Schlag, Chem. Phys. Lett. **32**, 210 (1975).
[37]R. J. Longfellow, D. B. Moss, and C. S. Parmenter, J. Phys. Chem. **92**, 5438 (1988).
[38]U. Schubert, E. Riedle, H. J. Neusser, and E. W. Schlag, J. Chem. Phys. **84**, 6182 (1986).